
QFT: Quantized Full-parameter Tuning of LLMs with Affordable Resources

Zhikai Li¹, Xiaoxuan Liu², Banghua Zhu², Zhen Dong²✉, Qingyi Gu¹✉, Kurt Keutzer²

¹Institute of Automation, Chinese Academy of Sciences ²University of California, Berkeley

{lizhikai2020, qingyi.gu}@ia.ac.cn

{xiaoxuan_liu, banghua, zhendong, keutzer}@berkeley.edu

Abstract

Large Language Models (LLMs) have showcased remarkable impacts across a wide spectrum of natural language processing tasks. Fine-tuning these pretrained models on downstream datasets provides further significant performance gains; however, this process typically requires a large number of expensive, high-end GPUs. Although there have been efforts focused on parameter-efficient fine-tuning, they cannot fully unlock the powerful potential of full-parameter fine-tuning. In this paper, we propose QFT, a Quantized Full-parameter Tuning framework for LLMs that quantizes and stores all training states, including weights, gradients, and optimizer states, in INT8 format to reduce training memory, thereby enabling full-parameter fine-tuning on existing GPUs at an affordable cost. To ensure training performance, we make two key efforts: i) for quantized gradients and optimizer states, we theoretically prove that the Lion optimizer, with its property of consistent update magnitudes, is highly robust to quantization; ii) and for quantized weights, we employ the hybrid feature quantizer, which identifies and protects a small subset of sparse critical features while quantizing the remaining dense features, thus ensuring accurate weight updates without FP32 backups. Moreover, to support backpropagation in the integer context, we develop a stack-based gradient flow scheme with $O(1)$ complexity, forming a unified integer training pipeline. As a result, QFT reduces the model state memory to 21% of the standard solution while achieving comparable performance, e.g., tuning a LLaMA-7B model requires only <30GB of memory, making it feasible on a single A6000 GPU.

1 Introduction

Large Language Models (LLMs), with up to hundreds of billions of parameters, have left an indelible mark on the landscape of natural language processing tasks, showcasing their remarkable impacts across a diverse spectrum of applications and domains [42, 43, 1, 47]. Fine-tuning these pre-trained models on downstream datasets enhances their ability to understand and perform specific tasks [49]. However, due to the enormous number of parameters, the fine-tuning process relies on massive and expensive GPU resources, resulting in extremely high costs.

Parameter-efficient fine-tuning (PEFT), which tunes only a subset of parameters, is considered a practical choice in low-resource settings [8, 15, 26, 46]. However, due to the limited representational capacity of the smaller parameter set, its performance often falls short of expectations [35, 48]. Consequently, we focus on full-parameter fine-tuning, with an emphasis on exploring memory optimization strategies to make it feasible on cost-effective resources.

We examine the full spectrum of memory usage in full-parameter fine-tuning, which can be categorized into three components: model states, activation, and other temporary or unusable memory,

✉ Corresponding authors.

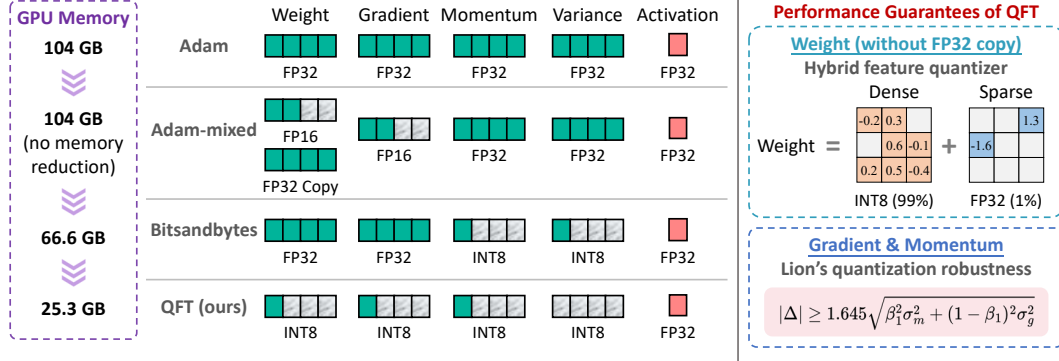


Figure 1: Comparison in GPU memory usage of different full-parameter fine-tuning methods, including standard FP32 Adam [22], mixed-precision FP16 Adam [36], BitsandBytes [6], and the proposed QFT. QFT significantly reduces training memory, enabling fine-tuning with affordable resources. To ensure the performance of quantized fine-tuning, QFT adopts the hybrid feature quantizer for weights, and for gradients and momentum, we theoretically prove that Lion exhibits high robustness to quantization, thereby ensuring comparable convergence to FP32 Adam.

as shown in Figure 1. Model states, which include weights, gradients, and optimizer states (e.g., momentum and variances in Adam [22]), consume the majority of the memory [39]. For instance, when employing the standard FP32 setting with Adam, the memory allocation for weights, gradients, momentum, and variances amounts to 4 times the number of parameters. As a result, tuning a LLaMA-7B model necessitates a minimum of 104GB of RAM, which presents a formidable challenge given the limitations of current GPU capacities. Notably, although mixed-precision training [36] reduces computation precision, it requires storing an additional FP32 weight copy, hence it only accelerates training but fails to address the memory consumption issues.

In this paper, we introduce QFT, a Quantized Full-parameter Tuning framework for training memory optimization. Specifically, QFT quantizes and stores all training states in INT8 format, significantly reducing memory consumption and enabling full-parameter fine-tuning on existing GPUs at an affordable cost. In contrast to traditional quantization-aware training (QAT), QFT focuses specifically on memory optimization by *storing* all parameters in low-bit format. To maintain training performance, we make two key efforts: **1 For quantized gradients and optimizer states**, we theoretically prove that the Lion optimizer [3], which tracks only momentum and produces consistent update magnitudes, exhibits strong robustness to quantization. Thus, we employ the Lion optimizer to minimize the effects of quantization of gradients and momentum. **2 For quantized weights**, we employ the hybrid feature quantizer, which selectively retains a small set of sparse critical features while quantizing the majority of dense features, thereby ensuring accurate weight updates. It does not rely on FP32 backups, thus achieving better memory efficiency than mixed-precision training. On this basis, to enable integer-based backpropagation, we design a stack-based gradient flow scheme with $O(1)$ complexity, constructing a unified integer training pipeline. It is also worth noting that QFT adopts the INT8 format by default, which is broadly supported by most hardware. This design avoids reliance on specialized data types like FP8 [37] that require high-end GPUs, thus enabling full utilization of existing mid- and low-end GPUs. Our contributions can be summarized as follows:

- We propose QFT, a Quantized Full-parameter Tuning framework for LLMs. It achieves training memory optimization by reducing storage precision, enabling full-parameter fine-tuning on affordable resources, which separates it from traditional QAT. In addition, QFT offers strong compatibility and can be seamlessly integrated into mainstream LLM training tools.
- To ensure training performance, we first theoretically prove the robustness of the Lion optimizer to quantization, thereby ensuring the reliability of *quantized gradients and optimizer states*. Then, we protect a small subset of critical features within the weights while quantizing the remaining dense features, effectively preserving the accuracy of *quantized weight updates*. Moreover, we develop a stack-based gradient flow scheme with $O(1)$ complexity to enable integer backpropagation.
- We perform instruction tuning on the pre-trained LLaMA-2 models and extensively evaluate performance on various benchmarks. The results demonstrate that our QFT, with memory usage reduced to 21%, achieves comparable performance to standard floating-point training.

2 Related Work

Efficient Optimizer The primary optimizers employed for training Transformer models are the Adam family [22, 33]. They maintain a rolling average of the previous gradients to promote stable convergence. However, their optimizer states (momentum and variances) imposes an extra memory overhead. To overcome the memory challenges of optimizer states, various memory-efficient strategies have been proposed. LOMO [35] utilizes vanilla SGD for LLM training, which unfortunately fails to ensure performance due to the slow convergence and weak stability of SGD [25]. BAdam [34] uses the block coordinate descent framework with Adam’s update rule to optimize memory. Another imperfect solution is Adafactor [41], which reduces memory usage by storing only aggregated information, yet remains prone to instability. In this work, we adopt the Lion optimizer [3], which tracks only momentum while achieving convergence performance comparable to Adam. More importantly, thanks to the sign operation, Lion ensures updates of consistent magnitude for each parameter, which gives it a great potential for robust quantization of gradients and optimizer states.

Quantization for Memory Optimization Most existing quantization methods focus on inference efficiency [13, 10, 9, 21, 28, 29, 27, 19], and recently, quantization is also believed to have great potential for training memory efficiency. Note that this research line differs from traditional QAT [19, 32]. QAT inserts fake quantization nodes on weights and activations during training, while the underlying parameter arithmetic and storage remain in floating-point format; thus, it does not improve training memory efficiency. In contrast, quantization-based memory optimization methods aim to leverage low-precision formats to *store* parameters, thereby effectively reducing memory consumption during training. For instance, Bitsandbytes [6] introduces a block-wise quantization strategy to compress the memory of optimizer states. QLoRA [7] uses quantized values to store frozen pre-training weights, keeping only the adapters in floating-point format. In this work, we focus on full-parameter fine-tuning and work to quantize all model states for comprehensive memory optimization without sacrificing fine-tuning performance.

Other Memory Optimization Methods Previous efforts have focused on optimizing the activation memory, including offloading [16, 44, 38] and gradient checkpointing [2, 24, 20, 23]. Activation offloading offloads activation to external memory, at the cost of transferring data to another storage (e.g., CPU memory). Gradient checkpointing discards activations in the forward pass and recomputes them in the backward pass as needed. In addition, there are also customized schemes for other states in training LLMs. GaLore [48] reduces the gradient memory by low-rank projection. LOMO [35] fuses the gradient computation and the parameter update in one step. This method can reduce the memory usage of gradient tensors to $O(1)$; however, there is a potential caveat as it is incompatible with gradient accumulation for scaling batch sizes, limiting it to unstable training with small batch sizes. In contrast, our framework is orthogonal and well compatible with all the above methods.

3 Methodology

In this paper, we propose a quantized fine-tuning framework to optimize training memory. We first theoretically prove in Section 3.1 that Lion provides strong robustness for quantized gradients and momentum. In Section 3.2, we introduce the hybrid feature quantizer for accurate weight updates. Finally, Section 3.3 presents the resulting integer training pipeline with stack-based gradient flow.

3.1 Lion Optimizer: Robust Quantization of Gradients and Momentum

In contrast to Bitsandbytes [6] which adopts advanced quantization strategies, we prioritize ease of use by applying the simplest uniform quantizer to gradients and momentum, defined as follows:

$$Quant : \mathbf{X}^{(\mathbb{Z})} = \text{clip} \left(\left\lfloor \frac{\mathbf{X}}{s} \right\rfloor + z, 0, 2^b - 1 \right), \quad De\text{-}quant : \hat{\mathbf{X}} = s \left(\mathbf{X}^{(\mathbb{Z})} - z \right) \approx \mathbf{X}, \quad (1)$$

where \mathbf{X} is the floating-point vector, $\mathbf{X}^{(\mathbb{Z})}$ is the quantized integer vector, $\lfloor \cdot \rfloor$ denotes the round function, and $b \in \mathbb{N}$ is the quantization bit-width. $s \in \mathbb{R}^+$ and $z \in \mathbb{Z}$ are the quantization scale and zero-point, which are determined by the arithmetic lower and upper bounds of \mathbf{X} as follows:

$$s = \frac{\max(\mathbf{X}) - \min(\mathbf{X})}{2^b - 1}, \quad z = \left\lfloor -\frac{\min(\mathbf{X})}{s} \right\rfloor. \quad (2)$$

The simplicity of the quantizer effectively ensures computational efficiency but also raises concerns about potential impacts on training performance. Fortunately, Lion [3] (detailed in Appendix A), which tracks only momentum and applies updates of consistent magnitude to each parameter via the sign operation, can significantly mitigate the adverse effects of quantization. More specifically, Lion has inherent advantages for quantized fine-tuning as follows:

- **Simplicity:** Lion only keeps track of the momentum, which saves memory by avoiding storing variances, while eliminating the potential effect of quantized variances.
- **Consistent Update Magnitudes:** Lion ensures that updates have the same magnitude for each parameter, which is determined through the sign operation. In a quantized setting, this consistency can mitigate potential imbalances or inaccuracies introduced by limited precision.

For the consistent update magnitude property, we provide a detailed proof below to demonstrate Lion's high robustness to quantization of gradients and momentum.

Assumption 1. Assume that:

- (Additive quantization error) The quantization error is additive, i.e., $\hat{x} = x + \delta_x$.
- (Bounded Gaussian error) The quantization error δ_x follows a Gaussian distribution $\mathcal{N}(0, \sigma_x^2)$, where σ_x^2 is small and bounded.

Lemma 1. Under Assumption 1, when quantizing gradients and momentum in Lion, if the increment Δ satisfies $|\Delta| \geq 1.645\sqrt{\beta_1^2\sigma_m^2 + (1 - \beta_1)^2\sigma_g^2}$, then with 95% probability, $\text{sign}(\Delta)$ remains invariant under quantization.

Proof. Given Assumption 1, we have:

$$\hat{m} = m + \delta_m, \quad \hat{g} = g + \delta_g, \quad \text{where } \delta_m \sim \mathcal{N}(0, \sigma_m^2), \quad \delta_g \sim \mathcal{N}(0, \sigma_g^2).$$

When quantizing gradients and momentum, the increment becomes:

$$\Delta' = \beta_1\hat{m} + (1 - \beta_1)\hat{g} = \Delta + \beta_1\delta_m + (1 - \beta_1)\delta_g.$$

Let $\delta_\Delta = \beta_1\delta_m + (1 - \beta_1)\delta_g$. Since δ_m and δ_g are independent Gaussian distributions, based on homogeneity and additivity, δ_Δ follows a Gaussian distribution:

$$\delta_\Delta \sim \mathcal{N}(0, \sigma_\delta^2) := \mathcal{N}(0, \beta_1^2\sigma_m^2 + (1 - \beta_1)^2\sigma_g^2).$$

To ensure that the sign of Δ remains invariant after quantization, we require that $\text{sign}(\hat{\Delta}) = \text{sign}(\Delta)$, i.e., Δ and $\Delta + \delta_\Delta$ must have the same sign. First, consider the case $\Delta > 0$, we require $\Delta + \delta_\Delta > 0 \Leftrightarrow \delta_\Delta > -\Delta$, thus the probability of sign preservation is:

$$P(\delta_\Delta > -\Delta) = 1 - P(\delta_\Delta \leq -\Delta).$$

Standardizing δ_Δ yields:

$$P(\delta_\Delta \leq -\Delta) = P\left(\frac{\delta_\Delta}{\sigma_\delta} \leq -\frac{\Delta}{\sigma_\delta}\right) = \Phi\left(-\frac{\Delta}{\sigma_\delta}\right),$$

where $\Phi(\cdot)$ denotes the cumulative distribution function of the standard normal distribution. To ensure the probability of sign flip is at most 5%, we require $\Phi\left(-\frac{\Delta}{\sigma_\delta}\right) \leq 0.05$. Since $\Phi^{-1}(0.05) = -1.645$, it follows that $-\frac{\Delta}{\sigma_\delta} \leq -1.645 \Leftrightarrow \Delta \geq 1.645\sigma_\delta$. Substituting σ_δ gives:

$$\Delta \geq 1.645\sqrt{\beta_1^2\sigma_m^2 + (1 - \beta_1)^2\sigma_g^2}.$$

Similarly, when both Δ and $(\Delta + \delta_\Delta)$ are negative, we have $\Delta \leq -1.645\sqrt{\beta_1^2\sigma_m^2 + (1 - \beta_1)^2\sigma_g^2}$.

Therefore, in summary, if $|\Delta| \geq 1.645\sqrt{\beta_1^2\sigma_m^2 + (1 - \beta_1)^2\sigma_g^2}$, then with at least 95% probability, $\text{sign}(\Delta)$ remains invariant under quantization, i.e., $\text{sign}(\hat{\Delta}) = \text{sign}(\Delta)$. \square

Remark 1. We empirically observe the ratio $\frac{|\Delta|}{\sigma_\delta}$ across different iterations and layers. Our results indicate that in at least 97.9% of cases, the ratio exceeds 1.645, thereby satisfying the condition stated above. Further details are provided in Appendix B.

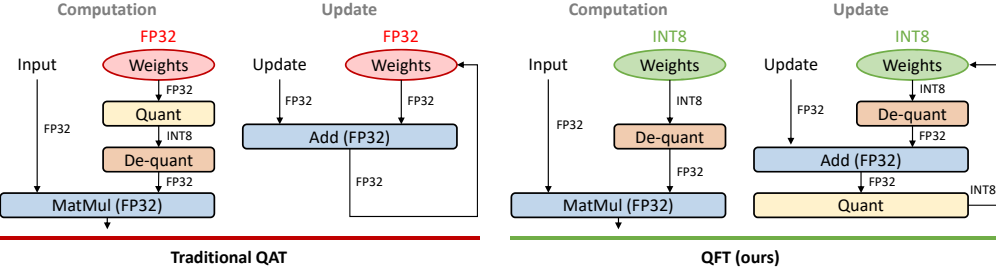


Figure 2: Comparison between our QFT and traditional QAT in the computation and update procedures of weights. QAT stores the weights in the floating-point format and adds fake quantization nodes to the computation. Conversely, in our QFT, the weights are stored in the low-precision integer format, which are de-quantized on-the-fly into the floating-point format for computation, resulting in a significant reduction in memory usage.

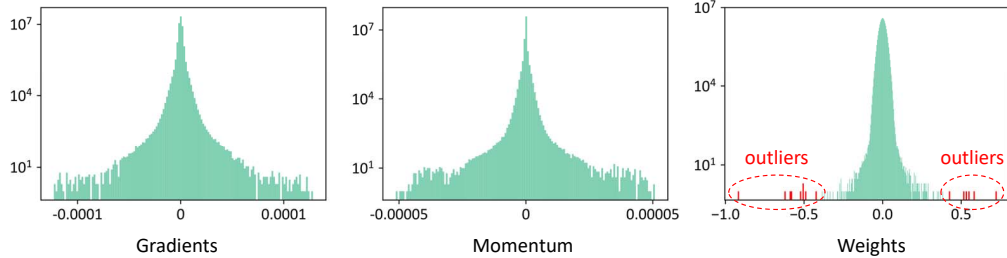


Figure 3: Illustration of the model state distributions when training a LLaMA-2-7B model. The weight values are from the final down projection layer, and the gradient and momentum values are fetched on the 200th training step. The gradients and momentum show a canonical centralized distribution with few outliers, while the range of the weights increases by three orders of magnitude and exhibits extreme outliers, posing a significant challenge.

3.2 Hybrid Feature Quantizer: Accurate Updates of Quantized Weights

In addition to gradients and momentum, we also store weights in integer format. It is important to note that this quantized storage procedure focuses on training memory optimization, and it is fundamentally different from traditional QAT [19] that inserts fake quantization nodes. In our framework, weights are *stored as quantized integers*, while computations are performed in de-quantized floating-point format, achieving significant memory reduction at the cost of a slight increase in computational overhead. Therefore, it follows the principle of trading a small amount of time for substantial space savings, and the comparison to QAT is illustrated in Figure 2.

However, weight quantization is significantly more challenging. In particular, we analyze the pattern of weight distributions and make two key observations: i) a small number of outliers exist in the weight distribution, and these outliers are shown to play a significant role in representation, typically corresponding to critical features [21, 11, 30]; and ii) these outliers negatively impact quantization by greatly expanding the numerical range of weights, which is approximately three orders of magnitude larger than that of momentum, as shown in Figure 3. These two conflicting properties make handling outliers particularly challenging.

Fortunately, the sparsity of outliers offers an opportunity to address the above challenge. Statistical analysis shows that 99% of the values are concentrated within only 20% of the overall range. This property motivates us to adopt the hybrid feature quantizer, inspired by SqueezeLLM [21]. It separates the top 1% of sparse critical features for preservation while compacting the distribution of dense features to enable effective quantization of the remaining values. Formally, the method is defined as follows:

$$\begin{aligned}
 \mathbf{W} &= \mathbf{D} + \mathbf{S}, \\
 \text{s.t. } \mathbf{D} &= \mathbf{W} \odot \mathbb{I}(T_{\min} \leq \mathbf{W} \leq T_{\max}), \\
 \mathbf{S} &= \mathbf{W} \odot \mathbb{I}(\mathbf{W} < T_{\min} \text{ or } \mathbf{W} > T_{\max}),
 \end{aligned} \tag{3}$$

where D is a dense matrix representing the centralized values, and S is a sparse matrix representing the outliers. Here, T_{\min} and T_{\max} are the thresholds for identifying outliers, and $\mathbb{I}(\cdot)$ is the indicator function. Note that the matrix decomposition process is numerically straightforward, ensuring a high level of computational efficiency with minimal repercussions on training overhead.

Subsequently, the dense matrix is quantized using the uniform quantizer described in Equation 1, while the sparse matrix retains its values in floating-point format. Notably, given that the outliers constitute a relatively minor fraction (1%), the sparse matrix can be stored using memory-efficient formats such as compressed sparse row, which significantly reduces memory overhead while preserving the integrity of the essential data structure.

Furthermore, QFT offers advantages over mixed-precision training, which requires maintaining an FP32 weight copy. In mixed-precision FP16 training, both forward and backward passes operate on FP16 weights and gradients; however, an FP32 copy of the weights must be used for updates. This is necessary because FP16, being a simple numerical truncation format, suffers from limited precision and potential overflow issues during weight updates. In contrast, unlike the rudimentary truncation in FP16, the quantization procedure in QFT preserves sparse critical features and, for dense features, maps FP32 values cohesively onto a set of uniformly distributed integer values. As a result, QFT achieves stable training without the need for maintaining an additional FP32 weight copy.

3.3 The Integer Training Pipeline

In this section, we integrate the above strategies to form a memory-efficient fine-tuning framework for LLMs. We provide a comprehensive description of each training phase, including forward propagation, backward propagation, and parameter update, with particular emphasis on the stack-based gradient flow scheme with $O(1)$ complexity in the integer context.

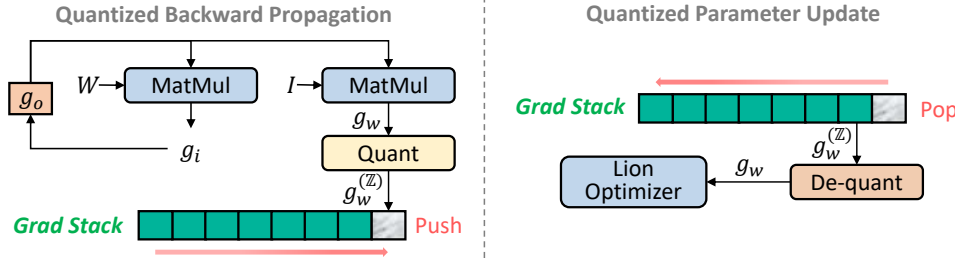


Figure 4: The proposed stack-based gradient flow scheme, which enables storage and $O(1)$ complexity access to integer gradients. This effectively eliminates AutoGrad’s dependency on floating-point formats, enabling efficient gradient propagation in the context of integer weights.

Quantized Forward Propagation Within our framework, we initially represent weights as quantized integer values to optimize memory utilization. During the execution of forward propagation, we de-quantize these low-precision weights into the floating-point format on-the-fly, thereby enabling high-precision arithmetic operations. For more clarity, we visualize this critical process in Figure 2.

Quantized Backward Propagation In the backward propagation phase, the final task loss is propagated forward from the last layer in a sequential manner, and throughout this process, the gradient of each parameter is computed. It’s worth noting that these gradients need to be kept in memory, as they serve as essential information for guiding subsequent updates to the parameters. However, in mainstream deep learning frameworks like PyTorch, only parameters in the floating-point format can possess the gradient property. Consequently, we cannot compute and store the gradients using the automatic differentiation functionality (i.e., AutoGrad) in such cases.

To this end, we design a new gradient flow in the context of integer weights, as illustrated in Figure 4 and detailed in Algorithm 1. As in forward propagation, we begin by de-quantizing the weights into floating-point format. Subsequently, leveraging the gradient of the output, we apply the chain rule to compute gradients with respect to both the input and the weights. Beyond computation, retaining weight gradients introduces additional challenges. To address this, we propose a gradient retention scheme based on a global stack structure. In this scheme, each layer’s gradient is sequentially pushed onto the stack, following the reverse order of information flow during backpropagation.

Algorithm 1 Gradient Flow of Quantized Weights

```
#  $T_l$  : saved tensors in forward pass of layer  $l$ 
#  $g_o$  : gradient of the current layer's output

 $S_g \leftarrow \text{stack}()$ 
for  $l = L, L-1, \dots, 1$  do
   $I_l, W_l^{(\mathbb{Z})} \leftarrow T_l$ 
   $W_l \leftarrow \text{dequant}(W_l^{(\mathbb{Z})})$ 
  calculate gradients of  $I_l$  and  $W_l$ 
   $g_i \leftarrow \text{matmul}(g_o, W_l)$ 
   $g_w \leftarrow \text{matmul}(g_o^T, I_l)$ 
   $g_w^{(\mathbb{Z})} \leftarrow \text{quant}(g_w)$             $\triangleright$  store as INT8
   $\text{push}(S_g, g_w^{(\mathbb{Z})})$             $\triangleright$  collect gradient
  assign  $g_o$  of layer (l-1)
   $g_o \leftarrow g_i$ 
end for
```

Algorithm 2 Quantized Lion Optimizer

```
#  $\beta_1, \beta_2, \lambda, \eta, f$  : optimizer parameters
#  $m_l$  : optimizer momentum of layer  $l$ 

for  $l = 1, 2, \dots, L$  do
   $g_w^{(\mathbb{Z})} \leftarrow \text{pop}(S_g)$             $\triangleright$  retrieve gradient
   $g_w \leftarrow \text{dequant}(g_w^{(\mathbb{Z})})$ 
   $m_l \leftarrow \text{dequant}(m_l^{(\mathbb{Z})})$ 
   $W_l \leftarrow \text{dequant}(W_l^{(\mathbb{Z})})$ 
  update model parameters
   $\Delta \leftarrow \beta_1 m_l + (1 - \beta_1) g_w$ 
   $W_l \leftarrow W_l - \eta(\text{sign}(\Delta) + \lambda W_l)$ 
  update EMA of  $g_w$ 
   $m_l \leftarrow \beta_2 m_l + (1 - \beta_2) g_w$ 
   $m_l^{(\mathbb{Z})} \leftarrow \text{quant}(m_l)$             $\triangleright$  store as INT8
   $W_l^{(\mathbb{Z})} \leftarrow \text{quant}(W_l)$             $\triangleright$  store as INT8
end for
```

Quantized Parameter Update Ultimately, the parameter update is performed following the standard Lion optimizer procedure, with the key distinction that both gradients and momentum are stored in integer format. The quantized optimizer step is described in Algorithm 2. First, gradients are retrieved by popping elements from the global stack, with constant-time complexity $O(1)$ regardless of the stack length. The efficiency arises from the design of the gradient flow: during backpropagation, gradients are sequentially pushed onto the stack starting from the last layer, and during the optimizer step, they are popped in order starting from the first layer. As a result, the gradient of the current layer is always on top of the stack, fully leveraging its first-in-last-out structure.

4 Experiments

4.1 Experimental Setup

Models and Benchmarks We conduct evaluation of the proposed QFT by fine-tuning LLaMA-2 [43], including the 7B and 13B versions. The few-shot performance of fine-tuned models is evaluated on various standard benchmarks, including ARC [5], HellaSwag [45], MMLU [14], and TruthfulQA [31]. All results are obtained using the Language Model Evaluation Harness tool [12]. In addition, we also use MT-Bench [50] with GPT-4 scores to evaluate the conversational abilities.

Dataset Preparation We use a dataset comprising 94.1K ShareGPT entries [18, 40], which capture user interactions with ChatGPT. Following FastChat [4], we convert HTML content to Markdown, remove non-English conversations, and split long dialogues into segments of up to 2048 tokens. For a fair comparison, all baseline methods are replicated using the same dataset as described above.

Baseline Methods We evaluate QFT in terms of both training memory and performance.

- For training memory, QFT is compared to standard FP32 Adam [22], mixed-precision FP16 Adam [36], BitsandBytes [6], and standard FP32 Lion [3].
- For training performance, we consider four baselines: **LoRA**, which is a PEFT method [15]; **FT-Adam**, which performs full-parameter fine-tuning using FP32 Adam [22]; **FT-Lion**, which performs full-parameter fine-tuning using FP32 Lion [3]; **FT-Bnb**, which uses Bitsandbytes [6] with quantized optimizer states for full-parameter fine-tuning.

Training Details The PEFT method LLaMA-2-LoRA follows the settings: the rank is 8, the alpha is 16, the dropout is 0.05, the learning rate is 2e-5, and the total number of epochs is 3. For full-parameter fine-tuning, all methods follow the same settings: the global batch size is 128, the learning rate is 2e-5, and the total number of epochs is 3. In QFT, we apply channel-wise quantization for all quantizers of model states. The threshold T in the dense-and-sparse quantizer is obtained from 1% of the distribution range (see Appendix C for details).

Table 1: Memory usage (in GB) when fine-tuning the LLaMA-2-7B model using different methods. We report the full spectrum of memory profiles, as well as the total allocated memory and peak allocated memory. QFT introduces quantization that reduces the memory to 21% of the Adam optimizer, allowing for fine-tuning within 30GB of RAM.

Method	Weights	Grads	Optimizer States			Activation	Total	Peak
			Weight Copies	Momentum	Variances			
Adam-FP32	25.1	25.1	-	25.1	25.1	3.75	104	129
Adam-FP16 mixed	12.6	12.6	25.1	25.1	25.1	3.75	104	123
Bitsandbytes	25.1	25.1	-	6.31	6.31	3.75	66.6	86.6
Lion-FP32	25.1	25.1	-	25.1	-	3.75	79.1	101
QFT (ours)	7.42	7.06	-	7.06	-	3.75	25.3	28.9

4.2 Memory Profile

We start by discussing the memory usage of different methods, as reported in Table 1. All experiments employ gradient checkpointing by default to reduce activation memory. Under standard Adam [22], each model state consumes 25.1GB of RAM. This issue persists in mixed-precision settings [36], where despite halving memory for weights and gradients, FP32 weight copies must be maintained to ensure stable updates. Lion [3] reduces memory usage by 25% by tracking only momentum. BitsandBytes [6] further compresses optimizer states via quantization, saving 37GB. However, the need to retain floating-point weights and gradients remains a limitation.

Our QFT, built on Lion, applies full quantization to all model states, requiring only 21.5GB of GPU memory, which is just 21% of that used by standard Adam. With activation memory included, the peak allocated memory stays below 30GB, enabling fine-tuning with limited computing resources.

4.3 Performance Evaluation

Training Throughput and Convergence We measure the average time per 1000 training steps. Due to quant-dequant overhead, QFT incurs a 1.2-1.3× increase in training time compared to LLaMA-2-FT with FP32 Adam. This time–memory trade-off is considered significant, especially under constrained memory budgets. Moreover, Figure 5 compares the training loss curves of QFT and LLaMA-2-FT, showing that QFT achieves comparable convergence.

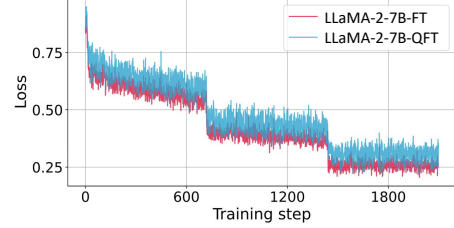


Figure 5: Comparison of training loss curves.

Few-Shot Evaluation We perform few-shot performance evaluation across a range of established benchmarks, with results presented in Table 2. For consistency, we adopt the same evaluation metrics as those used in the Open LLM Leaderboard [17]. When fine-tuning LLaMA-2-7B, QFT significantly boosts the average performance score from 54.4 to 57.4. Notably, QFT comes within 0.6 points of full-precision fine-tuning with Adam (FT-Adam), while substantially outperforming LoRA. We also provide a qualitative analysis in Appendix D.

MT-Bench Score We further adopt MT-Bench, an advanced benchmark designed to evaluate the conversational capabilities of LLMs. It comprises a series of challenging multi-turn, open-ended questions that closely reflect human conversational preferences, with GPT-4 serving as the automatic evaluator. The results are summarized in Table 3. For 7B models, LLaMA-2 achieves a modest score of 3.83. While LoRA yields a slight improvement, it still falls short by 0.97 compared to full-parameter fine-tuning. Notably, QFT closes this gap, achieving performance comparable to FT-Adam.

Table 3: MT-Bench scores using GPT-4, which can reflect model’s conversational abilities.

Pre-trained	Tuning	Full-param	MT-Bench Score
LLaMA-2-7B (Score: 3.83)	LoRA	✗	5.11
	FT-Adam	✓	6.08
	FT-Lion	✓	6.11
	FT-Bnb	✓	5.94
	QFT (ours)	✓	5.95
LLaMA-2-13B (Score: 4.69)	LoRA	✗	5.74
	FT-Adam	✓	6.46
	FT-Lion	✓	6.44
	FT-Bnb	✓	6.30
	QFT (ours)	✓	6.27

Table 2: Few-shot performance of different models on various standard benchmarks. Here, the number of shots is aligned to Open LLM Leaderboard [17]. We take LLaMA-2 as the baseline and compare the instruction tuning results. QFT achieves results comparable to FT-Adam and FT-Lion that employ full-precision full-parameter fine-tuning, with significant advantages over LoRA.

Pre-trained	Tuning	Full-param	ARC-c (25-shot)	HellaSwag (10-shot)	MMLU (5-shot)	TruthfulQA-mc (0-shot)	Average
LLaMA-2-7B	-	-	53.1	78.6	46.9	38.8	54.4
	LoRA	✗	53.0	78.0	47.8	45.8	56.2
	FT-Adam	✓	53.6	77.3	49.4	51.5	58.0
	FT-Lion	✓	53.5	77.6	49.2	51.3	57.9
	FT-Bnb	✓	53.1	76.9	49.0	51.1	57.5
LLaMA-2-13B	QFT (ours)	✓	52.9	76.7	48.8	51.1	57.4
	-	-	59.4	82.1	55.8	37.4	58.7
	LoRA	✗	57.3	81.2	55.6	44.7	59.7
	FT-Adam	✓	57.0	81.2	55.8	50.9	61.2
	FT-Lion	✓	56.6	81.2	55.6	50.7	61.0
LLaMA-2-13B	FT-Bnb	✓	56.0	80.9	55.4	49.4	60.4
	QFT (ours)	✓	56.2	81.0	55.9	48.6	60.4

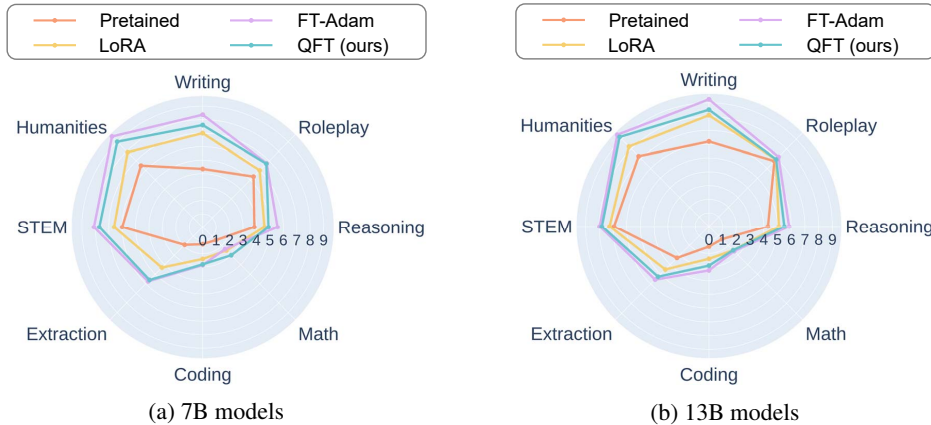


Figure 6: Radar charts of each capability in MT-Bench of different tuning method. QFT distinctly beats LoRA and achieves comparable results to FT-Adam.

We also provide radar charts covering eight capability dimensions, as shown in Figure 6. These visualizations demonstrate that QFT delivers comprehensive and consistent improvements across all evaluated metrics compared to the pre-trained LLaMA-2 baseline. Compared to FT-Adam, QFT achieves comparable performance and even surpasses it in specific areas, e.g., in the 7B setting, QFT exhibits superior performance in the Math metrics.

5 Conclusion

In this paper, we propose QFT, a memory-efficient framework for full-parameter fine-tuning of LLMs under quantized training settings. By quantizing all training states, including weights, gradients, and optimizer states, into INT8 format, QFT enables end-to-end training with significantly reduced memory consumption while preserving performance. We demonstrate two core techniques to ensure training performance: a quantization-robust optimizer (Lion) for momentum and gradients, and a hybrid feature quantizer that preserves sparse critical weight features. Furthermore, we introduce stack-based gradient flow with $O(1)$ complexity to support efficient integer-domain propagation. Empirical results show that QFT reduces model state memory usage to just 21% of standard FP32-based fine-tuning, allowing LLaMA-2-7B to be tuned on commodity GPUs (e.g., A6000 with <30GB memory). Our work highlights that full-parameter fine-tuning can be practical and affordable, opening new possibilities for broader adoption of LLM adaptation in resource-constrained environments.

References

- [1] Tom Brown, Benjamin Mann, Nick Ryder, Melanie Subbiah, Jared D Kaplan, Prafulla Dhariwal, Arvind Neelakantan, Pranav Shyam, Girish Sastry, Amanda Askell, et al. Language models are few-shot learners. *Advances in neural information processing systems*, 33:1877–1901, 2020.
- [2] Tianqi Chen, Bing Xu, Chiyuan Zhang, and Carlos Guestrin. Training deep nets with sublinear memory cost. *arXiv preprint arXiv:1604.06174*, 2016.
- [3] X Chen, C Liang, D Huang, E Real, K Wang, Y Liu, H Pham, X Dong, T Luong, CJ Hsieh, et al. Symbolic discovery of optimization algorithms. arxiv 2023. *arXiv preprint arXiv:2302.06675*, 2023.
- [4] Wei-Lin Chiang, Zhuohan Li, Zi Lin, Ying Sheng, Zhanghao Wu, Hao Zhang, Lianmin Zheng, Siyuan Zhuang, Yonghao Zhuang, Joseph E. Gonzalez, Ion Stoica, and Eric P. Xing. Vicuna: An open-source chatbot impressing gpt-4 with 90%* chatgpt quality, March 2023.
- [5] Peter Clark, Isaac Cowhey, Oren Etzioni, Tushar Khot, Ashish Sabharwal, Carissa Schoenick, and Oyvind Tafjord. Think you have solved question answering? try arc, the ai2 reasoning challenge. *arXiv preprint arXiv:1803.05457*, 2018.
- [6] Tim Dettmers, Mike Lewis, Sam Shleifer, and Luke Zettlemoyer. 8-bit optimizers via block-wise quantization. In *International Conference on Learning Representations*, 2021.
- [7] Tim Dettmers, Artidoro Pagnoni, Ari Holtzman, and Luke Zettlemoyer. Qlora: Efficient finetuning of quantized llms. *arXiv preprint arXiv:2305.14314*, 2023.
- [8] Ning Ding, Yujia Qin, Guang Yang, Fuchao Wei, Zonghan Yang, Yusheng Su, Shengding Hu, Yulin Chen, Chi-Min Chan, Weize Chen, et al. Delta tuning: A comprehensive study of parameter efficient methods for pre-trained language models. *arXiv preprint arXiv:2203.06904*, 2022.
- [9] Zhen Dong, Zhewei Yao, Daiyaan Arfeen, Amir Gholami, Michael W Mahoney, and Kurt Keutzer. Hawq-v2: Hessian aware trace-weighted quantization of neural networks. *Advances in neural information processing systems*, 33:18518–18529, 2020.
- [10] Zhen Dong, Zhewei Yao, Amir Gholami, Michael W Mahoney, and Kurt Keutzer. Hawq: Hessian aware quantization of neural networks with mixed-precision. In *Proceedings of the IEEE/CVF International Conference on Computer Vision*, pages 293–302, 2019.
- [11] Elias Frantar, Saleh Ashkboos, Torsten Hoefer, and Dan Alistarh. Gptq: Accurate post-training quantization for generative pre-trained transformers. *arXiv preprint arXiv:2210.17323*, 2022.
- [12] Leo Gao, Jonathan Tow, Stella Biderman, Sid Black, Anthony DiPofi, Charles Foster, Laurence Golding, Jeffrey Hsu, Kyle McDonell, Niklas Muennighoff, Jason Phang, Laria Reynolds, Eric Tang, Anish Thite, Ben Wang, Kevin Wang, and Andy Zou. A framework for few-shot language model evaluation, September 2021.
- [13] Amir Gholami, Sehoon Kim, Zhen Dong, Zhewei Yao, Michael W Mahoney, and Kurt Keutzer. A survey of quantization methods for efficient neural network inference. In *Low-Power Computer Vision*, pages 291–326. Chapman and Hall/CRC, 2022.
- [14] Dan Hendrycks, Collin Burns, Steven Basart, Andy Zou, Mantas Mazeika, Dawn Song, and Jacob Steinhardt. Measuring massive multitask language understanding. *arXiv preprint arXiv:2009.03300*, 2020.
- [15] Edward J Hu, Yelong Shen, Phillip Wallis, Zeyuan Allen-Zhu, Yuanzhi Li, Shean Wang, Lu Wang, and Weizhu Chen. Lora: Low-rank adaptation of large language models. *arXiv preprint arXiv:2106.09685*, 2021.
- [16] Chien-Chin Huang, Gu Jin, and Jinyang Li. Swapadvisor: Pushing deep learning beyond the gpu memory limit via smart swapping. In *Proceedings of the Twenty-Fifth International Conference on Architectural Support for Programming Languages and Operating Systems*, pages 1341–1355, 2020.
- [17] HuggingFace. Open llm leaderboard, 2023.
- [18] HuggingFace. Sharegpt data, 2023.

[19] Benoit Jacob, Skirmantas Kligys, Bo Chen, Menglong Zhu, Matthew Tang, Andrew Howard, Hartwig Adam, and Dmitry Kalenichenko. Quantization and training of neural networks for efficient integer-arithmetic-only inference. In *Proceedings of the IEEE conference on computer vision and pattern recognition*, pages 2704–2713, 2018.

[20] Paras Jain, Ajay Jain, Aniruddha Nrusimha, Amir Gholami, Pieter Abbeel, Joseph Gonzalez, Kurt Keutzer, and Ion Stoica. Checkmate: Breaking the memory wall with optimal tensor rematerialization. *Proceedings of Machine Learning and Systems*, 2:497–511, 2020.

[21] Sehoon Kim, Coleman Hooper, Amir Gholami, Zhen Dong, Xiuyu Li, Sheng Shen, Michael W Mahoney, and Kurt Keutzer. Squeezellm: Dense-and-sparse quantization. *arXiv preprint arXiv:2306.07629*, 2023.

[22] Diederik P Kingma and Jimmy Ba. Adam: A method for stochastic optimization. In *International Conference on Learning Representations*, 2015.

[23] Marisa Kirisame, Steven Lyubomirsky, Altan Haan, Jennifer Brennan, Mike He, Jared Roesch, Tianqi Chen, and Zachary Tatlock. Dynamic tensor rematerialization. *arXiv preprint arXiv:2006.09616*, 2020.

[24] Ravi Kumar, Manish Purohit, Zoya Svitkina, Erik Vee, and Joshua Wang. Efficient rematerialization for deep networks. *Advances in Neural Information Processing Systems*, 32, 2019.

[25] Bingrui Li, Jianfei Chen, and Jun Zhu. Memory efficient optimizers with 4-bit states. *arXiv preprint arXiv:2309.01507*, 2023.

[26] Xiang Lisa Li and Percy Liang. Prefix-tuning: Optimizing continuous prompts for generation. *arXiv preprint arXiv:2101.00190*, 2021.

[27] Zhikai Li and Qingyi Gu. I-vit: integer-only quantization for efficient vision transformer inference. *arXiv preprint arXiv:2207.01405*, 2022.

[28] Zhikai Li, Liping Ma, Mengjuan Chen, Junrui Xiao, and Qingyi Gu. Patch similarity aware data-free quantization for vision transformers. In *European Conference on Computer Vision*, pages 154–170. Springer, 2022.

[29] Zhikai Li, Junrui Xiao, Lianwei Yang, and Qingyi Gu. Repq-vit: Scale reparameterization for post-training quantization of vision transformers. *arXiv preprint arXiv:2212.08254*, 2022.

[30] Ji Lin, Jiaming Tang, Haotian Tang, Shang Yang, Xingyu Dang, and Song Han. Awq: Activation-aware weight quantization for llm compression and acceleration. *arXiv preprint arXiv:2306.00978*, 2023.

[31] Stephanie Lin, Jacob Hilton, and Owain Evans. Truthfulqa: Measuring how models mimic human falsehoods. *arXiv preprint arXiv:2109.07958*, 2021.

[32] Zechun Liu, Barlas Onguz, Changsheng Zhao, Ernie Chang, Pierre Stock, Yashar Mehdad, Yangyang Shi, Raghuraman Krishnamoorthi, and Vikas Chandra. Llm-qat: Data-free quantization aware training for large language models. *arXiv preprint arXiv:2305.17888*, 2023.

[33] Ilya Loshchilov and Frank Hutter. Decoupled weight decay regularization. *arXiv preprint arXiv:1711.05101*, 2017.

[34] Qijun Luo, Hengxu Yu, and Xiao Li. Badam: A memory efficient full parameter optimization method for large language models. *Advances in Neural Information Processing Systems*, 37:24926–24958, 2024.

[35] Kai Lv, Yuqing Yang, Tengxiao Liu, Qinghui Gao, Qipeng Guo, and Xipeng Qiu. Full parameter fine-tuning for large language models with limited resources. *arXiv preprint arXiv:2306.09782*, 2023.

[36] Paulius Micikevicius, Sharan Narang, Jonah Alben, Gregory Diamos, Erich Elsen, David Garcia, Boris Ginsburg, Michael Houston, Oleksii Kuchaiev, Ganesh Venkatesh, et al. Mixed precision training. *arXiv preprint arXiv:1710.03740*, 2017.

[37] Paulius Micikevicius, Dusan Stosic, Neil Burgess, Marius Cornea, Pradeep Dubey, Richard Grisenthwaite, Sangwon Ha, Alexander Heinecke, Patrick Judd, John Kamalu, et al. Fp8 formats for deep learning. *arXiv preprint arXiv:2209.05433*, 2022.

[38] Xuan Peng, Xuanhua Shi, Hulin Dai, Hai Jin, Weiliang Ma, Qian Xiong, Fan Yang, and Xuehai Qian. Capuchin: Tensor-based gpu memory management for deep learning. In *Proceedings of the Twenty-Fifth International Conference on Architectural Support for Programming Languages and Operating Systems*, pages 891–905, 2020.

[39] Samyam Rajbhandari, Jeff Rasley, Olatunji Ruwase, and Yuxiong He. Zero: Memory optimizations toward training trillion parameter models. In *SC20: International Conference for High Performance Computing, Networking, Storage and Analysis*, pages 1–16. IEEE, 2020.

[40] shareGPT. Sharegpt, 2023.

[41] Noam Shazeer and Mitchell Stern. Adafactor: Adaptive learning rates with sublinear memory cost. In *International Conference on Machine Learning*, pages 4596–4604. PMLR, 2018.

[42] Hugo Touvron, Thibaut Lavril, Gautier Izacard, Xavier Martinet, Marie-Anne Lachaux, Timothée Lacroix, Baptiste Rozière, Naman Goyal, Eric Hambro, Faisal Azhar, et al. Llama: Open and efficient foundation language models. *arXiv preprint arXiv:2302.13971*, 2023.

[43] Hugo Touvron, Louis Martin, Kevin Stone, Peter Albert, Amjad Almahairi, Yasmine Babaei, Nikolay Bashlykov, Soumya Batra, Prajjwal Bhargava, Shruti Bhosale, et al. Llama 2: Open foundation and fine-tuned chat models. *arXiv preprint arXiv:2307.09288*, 2023.

[44] Linnan Wang, Jinmian Ye, Yiyang Zhao, Wei Wu, Ang Li, Shuaiwen Leon Song, Zenglin Xu, and Tim Kraska. Superneurons: Dynamic gpu memory management for training deep neural networks. In *Proceedings of the 23rd ACM SIGPLAN symposium on principles and practice of parallel programming*, pages 41–53, 2018.

[45] Rowan Zellers, Ari Holtzman, Yonatan Bisk, Ali Farhadi, and Yejin Choi. Hellaswag: Can a machine really finish your sentence? *arXiv preprint arXiv:1905.07830*, 2019.

[46] Jun Zhang, Jue WANG, Huan Li, Lidan Shou, Ke Chen, Yang You, Guiming Xie, Xuejian Gong, and Kunlong Zhou. Train small, infer large: Memory-efficient loRA training for large language models. In *The Thirteenth International Conference on Learning Representations*, 2025.

[47] Susan Zhang, Stephen Roller, Naman Goyal, Mikel Artetxe, Moya Chen, Shuohui Chen, Christopher Dewan, Mona Diab, Xian Li, Xi Victoria Lin, et al. Opt: Open pre-trained transformer language models. *arXiv preprint arXiv:2205.01068*, 2022.

[48] Jiawei Zhao, Zhenyu Zhang, Beidi Chen, Zhangyang Wang, Anima Anandkumar, and Yuandong Tian. Galore: Memory-efficient llm training by gradient low-rank projection. *arXiv preprint arXiv:2403.03507*, 2024.

[49] Wayne Xin Zhao, Kun Zhou, Junyi Li, Tianyi Tang, Xiaolei Wang, Yupeng Hou, Yingqian Min, Beichen Zhang, Junjie Zhang, Zican Dong, et al. A survey of large language models. *arXiv preprint arXiv:2303.18223*, 2023.

[50] Lianmin Zheng, Wei-Lin Chiang, Ying Sheng, Siyuan Zhuang, Zhanghao Wu, Yonghao Zhuang, Zi Lin, Zhuohan Li, Dacheng Li, Eric Xing, et al. Judging llm-as-a-judge with mt-bench and chatbot arena. *arXiv preprint arXiv:2306.05685*, 2023.

A The Standard Lion Procedure

Here, we show the standard Lion procedure with full-precision calculations in Algorithm 3.

Algorithm 3 Lion Optimizer

```

given  $\beta_1, \beta_2, \lambda, \eta, f$ 
initialize  $\theta_0, m_0 \leftarrow 0$ 
for  $t = 1, 2, \dots, T$  do
     $g_t \leftarrow \nabla_\theta f(\theta_{t-1})$ 
    update model parameters
     $c_t \leftarrow \beta_1 m_{t-1} + (1 - \beta_1) g_t$ 
     $\theta_t \leftarrow \theta_{t-1} - \eta(\text{sign}(c_t) + \lambda \theta_{t-1})$ 
    update EMA of  $g_t$ 
     $m_t \leftarrow \beta_2 m_{t-1} + (1 - \beta_2) g_t$ 
end for
return  $\theta_t$ 

```

B Analysis of Values of $\frac{|\Delta|}{\sigma_\delta}$

Lemma 1 shows when $|\Delta| \geq 1.645 \sqrt{\beta_1^2 \delta_m^2 + (1 - \beta_1)^2 \delta_g^2}$, there is a 95% probability that $\text{sign}(\Delta)$ is invariant to quantization. Here, we experimentally verify that the condition hold well. Specifically, we sample $\frac{|\Delta|}{\sigma_\delta}$ in different iterations of different layers. σ_δ is obtained by maximum likelihood estimation based on the observed value. The results are presented in Table 4. As we can see, at least 97.9% of cases are greater than 1.645, satisfying the above condition. We also randomly select 1000 samples and visualize their values, as shown in Figure 7.

Table 4: Percentage distribution of $\frac{|\Delta|}{\sigma_\delta}$ in different iterations of different layers. We can see that more than 97.9% of cases are greater than 1.645.

Layer	Iteration	$\frac{ \Delta }{\sigma_\delta} < 1.645$	$\frac{ \Delta }{\sigma_\delta} \geq 1.645$
0	200	1.6%	98.4%
	1200	1.3%	98.7%
15	200	1.1%	98.8%
	1200	1.1%	98.9%
31	200	2.1%	97.9%
	1200	1.9%	98.1%

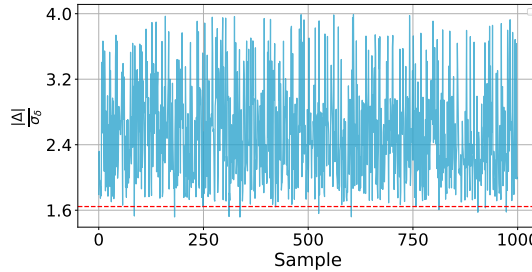


Figure 7: Display of 1000 samples sampled at the 200th training step of the final down projection layer.

C Discussion on Outlier Thresholds of Weight Quantizer

In this section, we discuss the selection and updating strategies for outlier thresholds in dense-and-sparse quantizers. We first report the memory and accuracy of dense-and-sparse quantizers using different percentage thresholds, and the results are shown in Table 5. The accuracy, i.e., the degree of distributional approximation of the quantizers, is evaluated by L_2 distance between de-quantized weights $\hat{\mathbf{W}}$ and full-precision weights \mathbf{W} , where the quantized weights are from the final down projection layer.

Table 5: Comparison of memory (in GB) and accuracy of dense-and-sparse quantizers using different percentage thresholds for weights. Here, accuracy is measured by L_2 distance between de-quantized $\hat{\mathbf{W}}$ and full-precision \mathbf{W} .

Percentile	0	0.45%	1.0%	3.0%	5.0%
Memory	7.06	7.23	7.42	8.23	9.16
L_2 Distance	436	0.846	0.619	0.566	0.479

The benefits of employing matrix decomposition in dense-and-sparse quantizers are readily evident from the results. When the percentile is set to 0, the quantizer no longer filters out the outliers and degenerates into a standard uniform quantizer, resulting in intolerable quantization errors. A noteworthy value suggested in SqueezeLLM [21] is 0.45%. However, it's essential to acknowledge that this tight bound is primarily designed for inference scenarios. To accommodate potential fluctuations during training, some level of relaxation in the thresholds is necessary. To this end, we assess the relaxed constraints at percentiles of 1.0%, 3.0%, and 5.0%. The findings reveal that, although the 3% and 5% percentiles yield a slight boost in accuracy, they also incur higher memory usage. Consequently, we advocate for the 1% percentile as a more favorable choice for achieving a balance between memory conservation and accuracy.

We also explore the update frequency of the thresholds. In order to maintain a high training throughput, we adopt a strategy of lazy updates, meaning that the thresholds set in the first iteration are reused in subsequent iterations. This approach is viable due to the smooth numerical updates of the weights during the fine-tuning process across neighboring iterations. Additionally, to our surprise, we discover that the initial thresholds remain effective for an entire epoch. As a result, we only update the thresholds once at the beginning of each epoch.

D Qualitative Analysis of Conversational Abilities

In the experimental section, we demonstrate the effectiveness of QFT through quantitative evaluations of LLMs' performance on a variety of benchmarks. Despite the large number of benchmarks, the results of the machine evaluations are not considered to be comprehensive, and in some cases, their reliability may be subject to scrutiny, e.g., the "shortcut" issue. Consequently, in the following, we intuitively show and compare examples generated by LLMs, aiming to further verify the conversational abilities through qualitative analysis.

[Writing Ability]

Question: Write a captivating movie review for a recently released science fiction film, discussing its plot, characters, and special effects.

LLaMA-2-7B-FT-Adam: "The Last Voyage" is a thrilling science fiction film that follows a group of astronauts on a mission to explore a distant planet. When they arrive, they discover that the planet is inhabited by a mysterious alien race. As they try to communicate with the aliens and gather data, they realize that their mission may be more dangerous than they ever imagined. With stunning special effects and a gripping plot, "The Last Voyage" is a must-see for science fiction fans.

LLaMA-2-7B-QFT: "Intergalactic Intrigue" is a thrilling science fiction film that takes viewers on a journey through the stars. The film follows a group of space explorers as they embark on a mission to uncover the secrets of an ancient alien civilization. The film's special effects are top-notch, with stunning visuals that transport viewers to a world of wonder and discovery. The characters

are well-developed and likable, with each member of the crew bringing their own unique skills and personalities to the table.

[Roleplay Ability]

Question: As a superhero, how would you explain your origin story to a curious child?

LLaMA-2-7B-FT-Adam: I was just like any other kid, until one day I was exposed to a strange chemical that gave me incredible powers. I learned to control the elements and use them to protect the innocent. I became known as the Elemental Guardian, and I've been fighting crime and saving the day ever since.

LLaMA-2-7B-QFT: I was just like any other kid, playing in the park and having fun. But one day, I was hit by a strange ray that gave me superpowers. I could fly, turn invisible, and even control the weather! I decided to use my powers to help people and fight crime. That's how I became the superhero you know and love!

[Common-sense Ability]

Question: In a world where automation is becoming increasingly prevalent, is it more important to prioritize job creation or technological progress?

LLaMA-2-7B-FT-Adam: Job creation is essential for a thriving economy, as it provides individuals with employment opportunities and a source of income. While technological progress is important for driving innovation and improving efficiency, it is crucial to balance technological advancements with the creation of new jobs. This can be achieved by investing in education and training programs that help workers develop the skills necessary to adapt to new technologies and by promoting policies that support small businesses and entrepreneurship. By prioritizing both job creation and technological progress, we can ensure a more stable and prosperous future for all.

LLaMA-2-7B-QFT: In the short term, job creation is a critical concern for policymakers and businesses. The unemployment rate remains high, and many people are struggling to find work. However, in the long term, technological progress is essential for driving economic growth and improving the standard of living for everyone. Automation has the potential to increase productivity and efficiency, which can lead to higher wages and better working conditions for employees. However, it can also lead to job displacement, particularly in industries where automation is most prevalent.

[Fermi Ability]

Question: How many snowflakes fall during a typical winter? Try to explain your answer. Your explanation should take the reader through your reasoning step-by-step.

LLaMA-2-7B-FT-Adam: It is difficult to determine the average number of snowflakes that fall during a typical winter, as it can vary greatly depending on location, climate, and other factors. However, it is estimated that on average, a single snowflake can have up to 100,000 ice crystals per flake. Over the course of a typical winter, this could result in billions of snowflakes falling from the sky.

LLaMA-2-7B-QFT: To answer this question, we need to consider the average snowfall for a typical winter in a given location. In the United States, for example, snowfall tends to be heaviest in the northern states, where the average snowfall for a typical winter is around 60 inches. In the southern states, snowfall is much less common and the average snowfall for a typical winter is around 10 inches.

[Counterfactual Ability]

Question: What if the Internet had been invented during the Renaissance period?

LLaMA-2-7B-FT-Adam: The Renaissance would have been a much different time period if the internet had been invented. The flow of information would have been much faster and more efficient, leading to a greater exchange of ideas and innovations. The world would have been connected in ways never before seen, allowing for the rapid spread of new ideas and technologies.

LLaMA-2-7B-QFT: The Renaissance was characterized by a renewed interest in classical learning and the arts, and the Internet would have provided a way for people to access and share this knowledge. It would have also facilitated the exchange of ideas and the development of new technologies, leading to even greater advancements in the fields of science, medicine, and engineering.

[Generic Ability]

Question: Can you explain the basics of quantum computing?

LLaMA-2-7B-FT-Adam: Quantum computing is a type of computing that uses quantum bits (qubits) to perform calculations, unlike traditional computers that use binary.

LLaMA-2-7B-QFT: Quantum computing is a type of computing that uses quantum-mechanical phenomena, such as superposition and entanglement, to perform operations on data. These phenomena allow quantum computers to perform certain calculations much faster than classical computers.

[Knowledge Ability]

Question: Explain the process of natural selection and how it contributes to the evolution and adaptation of species.

LLaMA-2-7B-FT-Adam: Natural selection is the process by which species adapt to their environment through the survival and reproduction of individuals with favorable traits. Over time, these favorable traits become more common in the population, leading to the evolution of new species.

LLaMA-2-7B-QFT: Natural selection is a process where species that are better adapted to their environment tend to survive and reproduce more than those that are less adapted. This leads to the survival of the fittest and the gradual evolution of species over time.